WIRELESS COMMUNICATIONS AND MOBILE COMPUTING
Wirel. Commun. Mob. Comput. 2012; **12**:1037–1052
Published online 22 September 2010 in Wiley Online Library (wileyonlinelibrary.com). DOI: 10.1002/wcm.1029

RESEARCH ARTICLE

Fundamental limits and improved algorithms for linear least-squares wireless position estimation†

Ismail Guvenc[1]*, Sinan Gezici[2] and Zafer Sahinoglu[3]

[1] DOCOMO Communications Laboratories USA, Inc., 3240 Hillview Avenue, Palo Alto, CA 94304, USA
[2] Department of Electrical and Electronics Engineering, Bilkent University, Bilkent, Ankara 06800, Turkey
[3] Mitsubishi Electric Research Labs, 201 Broadway, Cambridge, MA 02139, USA

ABSTRACT

In this paper, theoretical lower bounds on performance of linear least-squares (LLS) position estimators are obtained, and performance differences between LLS and nonlinear least-squares (NLS) position estimators are quantified. In addition, two techniques are proposed in order to improve the performance of the LLS approach. First, a reference selection algorithm is proposed to optimally select the measurement that is used for linearizing the other measurements in an LLS estimator. Then, a maximum likelihood approach is proposed, which takes correlations between different measurements into account in order to reduce average position estimation errors. Simulations are performed to evaluate the theoretical limits and to compare performance of various LLS estimators. Copyright © 2010 John Wiley & Sons, Ltd.

KEYWORDS

wireless positioning; time-of-arrival (TOA); least-squares (LS) estimation; maximum likelihood (ML); Cramer–Rao lower bound (CRLB)

***Correspondence**

Ismail Guvenc, DOCOMO Communications Laboratories USA, Inc., 3240 Hillview Avenue, Palo Alto, CA 94304, USA.
E-mail: iguvenc@docomolabs-usa.com

1. INTRODUCTION

In wireless networks, position information not only facilitates various applications and services [1–4] but also improves performance of communications systems by means of location-aware algorithms [5–7]. For a scenario in which a number of fixed terminals (FTs) with known positions are trying to estimate the position of a mobile terminal (MT), wireless position estimation is commonly performed in two steps [2]. In the first step, various measurements are first performed between the MT and the FTs, which carry information about the MT position. Those measurements can be based, for example, on time-of-arrival (TOA), received-signal-strength (RSS), and angle-of-arrival (AOA) estimation [1]. Then, in the second step, the MT position is estimated based on the measurements (estimates) obtained in the first step. In this step, mapping (fingerprinting), geometric, or statistical approaches can be followed. Since the mapping approach is based on a training data, which may not always be available, and the geometric techniques are not robust against noise, the statistical approach is commonly employed in position estimation [2]. Among the statistical techniques, the nonlinear least-squares (NLS) estimator can be applied in various scenarios [1,8]. The main justification for the use of the NLS estimator is that it provides the maximum likelihood (ML) solution, and can perform closely to theoretical limits, namely, Cramer–Rao lower bounds (CRLBs), for independent zero-mean Gaussian noise components at various measurements, which is commonly valid for line-of-sight (LOS) scenarios [1,3,9]. In addition, with various modifications, the NLS estimator can also have reasonable performance in certain non-line-of-sight (NLOS) scenarios [8,10–12].

The NLS estimation requires the minimization of a cost function that requires numerical search methods such as the Gauss-Newton and the steepest descent techniques, which can have high computational complexity and typically require sufficiently good initialization in order to avoid converging to local minima of the cost function [8]. In order to avoid the computational complexity of the NLS approach, various modifications to the NLS estimator are considered [13–16]. In Reference [13], the set of expressions corre-

†Part of this work was presented at the IEEE Wireless Communications and Networking Conference (WCNC) 2008 and at the IEEE International Conference on Communications (ICC) 2008.

sponding to the position related parameter estimates are linearized using the Taylor series expansion. However, this technique still requires an intermediate position estimate to obtain the Jacobian matrix, which should be sufficiently close to the true MT position for the linearity assumption to hold. Another approach is to obtain linearized expressions, by using one measurement as a reference for the other ones, and to obtain the position estimate *via* a linear least-squares (LLS) approach [14]. Various versions of the LLS approach are studied in References [15] and [16], which determine reference measurements in different manners (*cf.* Section 3).

The main advantage of the LLS approach is that it provides a simple closed-form and low-complexity solution for the MT position. However, it is not an optimal estimator, and has lower accuracy than the NLS approach in general. Therefore, it is well suited for applications that require low cost/complexity implementation with reasonable positioning accuracy. As will be demonstrated in Section 5 through computer simulations, accuracy of the LLS approach becomes even closer to the fundamental lower bounds with the proposed improvements, which may be sufficient for many applications. In addition, for applications that require accurate position estimation, the LLS approach can be used to obtain an initial position estimate for initializing high-accuracy position estimation algorithms, such as the NLS approach and linearization based on the Taylor series [17]. A good initialization can reduce computational complexity and position estimation errors of such high-accuracy techniques.

The aim of this paper is to quantify, *via* CRLB derivations, the amount of optimality loss induced by the linearization operations in LLS estimators, and propose new LLS algorithms in order to improve the performance of the LLS approach. Although theoretical mean-squared errors (MSEs) of the LLS estimator in Reference [14] are derived for various scenarios in References [18,19], no studies have considered generic theoretical lower bounds for LLS estimators that utilize linearized measurements. In this paper, first, the CRLB for the LLS estimator in Reference [14] is derived. Then, it is shown that this CRLB expression is also valid for various LLS estimators proposed in the literature [15,16]. After quantifying the optimality loss of the prior-art LLS estimators, two techniques are proposed in order to improve the performance of the LLS approach. First, *reference selection* is proposed for the LLS estimator in Reference [14], and then an ML approach is applied to the linearized measurements in order to take the correlations of various measurements into account. Simulation results are provided to evaluate the theoretical limits and to analyze performance of the proposed algorithms.

The remainder of the paper is organized as follows. In Section 2, the system model is defined, and the NLS estimation and the related CRLB are briefly reviewed. In Section 3, the conventional LLS estimators [14–16] are studied and the CRLB on their performance is derived. Then, improvements over the conventional LLS estimators are proposed *via* reference selection and ML estimation techniques in Section 4. Finally, the simulation results are presented in Section 5, followed by the concluding remarks in Section 6.

2. SYSTEM MODEL AND NONLINEAR LS ESTIMATION

A wireless system with N FTs are considered, where the location of the ith FT is denoted by $\boldsymbol{l}_i = [x_i \; y_i]^{\mathrm{T}}$, for $i = 1, 2, \ldots, N$, in a two-dimensional positioning scenario[‡]. A conventional two-step position estimation approach is adopted, where the first step obtains estimates of position related parameters at each FT, and then the second step calculates the estimate of the MT position based on the parameter estimates obtained in the first step [2]. In this paper, positioning systems that provide distance ('range') estimates in the first step are considered. Note that the range estimates may be obtained, for example, based on the TOA or the RSS metrics estimated at each FT [3].

The distance measurement (estimate) at the ith FT can be modeled as

$$z_i = f_i(x, y) + n_i, \qquad i = 1, \ldots, N \tag{1}$$

where n_i is the noise in the ith measurement, and $f_i(x, y)$ is the true distance between the MT and the ith FT, given by

$$f_i(x, y) = \sqrt{(x - x_i)^2 + (y - y_i)^2}, \tag{2}$$

with $\boldsymbol{l} = [x \; y]^{\mathrm{T}}$ denoting the unknown position of the MT.

Depending on the amount of information on the noise statistics and the availability of prior statistical information about the position of the MT, various estimators can be derived for estimating the MT position. When the probability density function (PDF) of the noise and the prior distribution of the MT position are known, Bayesian estimators, such as minimum mean-squared error (MMSE) estimator, can be obtained [2]. However, in many situations, no prior information on the MT position is available. In such cases, ML estimators can be employed, which estimate the MT position by maximizing the likelihood function for the position parameter [2].

The specific form of an ML estimator for the position of an MT depends on the joint PDF of the noise components in Equation (1). When the MT has direct line-of-sight (LOS) with all the FTs, the noise components are commonly modeled as independent zero-mean Gaussian random variables [1]. In this case, the ML estimator is given by

$$\hat{\boldsymbol{l}} = \left[\hat{x}\hat{y}\right]^{\mathrm{T}} = \arg\min_{(x,y)} \sum_{i=1}^{N} \beta_i (z_i - f_i(x, y))^2 \tag{3}$$

[‡] The results in this paper can also be extended to three-dimensional positioning scenarios.

where $\beta_i = 1/\sigma_i^2$ represents a weighting coefficient for the ith measurement, with σ_i^2 representing the error variance of the measurement related to the ith FT. The estimator in Equation (3) is referred to as the NLS estimator and is commonly used in position estimation [1,2].

When the direct LOS between the MT and an FT is blocked, i.e., in NLOS conditions, the corresponding distance measurement is corrupted by noise that can have significantly different PDF from a zero-mean Gaussian random variable [20,21]. Specifically, NLOS situations can cause a bias in distance estimation; hence, the related noise components commonly have positive mean values [1]. Although the NLS estimator in Equation (3) is not the ML solution for non-Gaussian noise components, it is commonly employed for position estimation in the absence of sufficient statistical information about the noise components. In that case, β_i is considered more generally as a *reliability* weight for the ith distance measurement, which takes a larger value as the accuracy of the measurement increases[§] [1]. In addition, in the presence of information about the mean of the noise (bias) in NLOS scenarios, the NLS estimator can be modified as [3]

$$\hat{\boldsymbol{l}} = \left[\hat{x}\hat{y}\right]^{\mathrm{T}} = \arg\min_{(x,y)} \sum_{i=1}^{N} \beta_i \left(z_i - \hat{b}_i - f_i(x,y)\right)^2 \quad (4)$$

where $\hat{b}_i$ is the estimate of the bias in the ith distance measurement. Finally, when the distance measurements related to the NLOS FTs can be identified, for example, by one of the algorithms proposed in References [22–24], the NLS estimator in Equation (3) can be employed based on the distance measurements related to the LOS FTs only (if there is a sufficient number of them).

Because the NLS estimator can be employed in various scenarios and it is the ML estimator for independent zero-mean Gaussian noise components, it is of interest to investigate its theoretical limits. Since an ML estimator asymptotically achieves the CRLB under certain conditions [9], the NLS estimator can provide an asymptotically optimal estimator under the stated conditions.

Based on the measurements model in Equation (1) with independent zero-mean Gaussian noise components, the CRLB for an unbiased NLS $\hat{\boldsymbol{l}}$ can be expressed as[‖]

$$\mathrm{Cov}\left\{\hat{\boldsymbol{l}}\right\} \geq \mathbf{I}^{-1} \quad (5)$$

with the following Fisher information matrix (FIM),

$$\mathbf{I} = \begin{bmatrix} \sum_{i=1}^{N} \frac{(x-x_i)^2}{\sigma_i^2 f_i^2(x,y)} & \sum_{i=1}^{N} \frac{(x-x_i)(y-y_i)}{\sigma_i^2 f_i^2(x,y)} \\ \sum_{i=1}^{N} \frac{(x-x_i)(y-y_i)}{\sigma_i^2 f_i^2(x,y)} & \sum_{i=1}^{N} \frac{(y-y_i)^2}{\sigma_i^2 f_i^2(x,y)} \end{bmatrix} \quad (6)$$

where σ_i^2 denotes the variance of the noise in the ith measurement [9,25,26]. Then, the lower bound on the MSE can be calculated as

$$\mathrm{MSE} = \mathrm{E}\{\|\hat{\boldsymbol{l}} - \boldsymbol{l}\|^2\} \geq \mathrm{trace}\{\mathbf{I}^{-1}\} = \frac{\mathrm{I}_{11} + \mathrm{I}_{22}}{\mathrm{I}_{11}\mathrm{I}_{22} - \mathrm{I}_{12}^2} \quad (7)$$

where I_{ij} represents the element of matrix $\mathbf{I}$ in the ith row and jth column, and $\mathrm{I}_{11} + \mathrm{I}_{22}$ is equal to $\sum_{i=1}^{N} \sigma_i^{-2}$.

As the NLS estimator in Equation (3) can asymptotically achieve the MMSE in Equation (7) under certain conditions, it provides a benchmark for the performance of other estimators. The main disadvantage of the NLS estimator is related to the nonlinear cost function for the minimization problem, which increases the computational complexity. The main techniques for obtaining the NLS solution in Equation (3) include gradient descent algorithms and linearization techniques *via* the Taylor series expansion [1,13].

3. LINEAR LS APPROACHES AND THEORETICAL LIMITS

3.1. Linear LS estimation

The high computational complexity of the NLS approach is mainly due to the nonlinear cost function, the minimization of which requires computation-intensive operations. In order to provide a low complexity solution to the position estimation problem, various LLS estimators are proposed in References [14–16,27]. The main idea behind the LLS approach is to obtain a set of linear equations from the nonlinear relations in Equations (1) and (2) *via* simple addition and subtraction operations.

In order to comprehend the linearization process, one can first consider the noiseless version of Equations (1) and (2), which can be expressed as

$$z_i^2 = (x - x_i)^2 + (y - y_i)^2, \qquad i = 1, \ldots, N \quad (8)$$

Then, one of those equations, say the rth one, is selected as the *reference* and subtracted from all the other equations, which results, after some manipulation [27], in the following linear relation:

$$\mathbf{A}_r \boldsymbol{l} = \mathbf{p}_r \quad (9)$$

where $\boldsymbol{l} = [x\ y]^{\mathrm{T}}$ is the MT position to be estimated,

$$\mathbf{A}_r = 2 \begin{bmatrix} x_1 - x_r & \cdots & x_{r-1} - x_r & x_{r+1} - x_r & \cdots & x_N - x_r \\ y_1 - y_r & \cdots & y_{r-1} - y_r & y_{r+1} - y_r & \cdots & y_N - y_r \end{bmatrix}^{\mathrm{T}} \quad (10)$$

[§] Accuracy of the ith distance measurement can be deduced, for example, from the history of measurements related to the ith FT.

[‖] Note that the CRLB is valid for all unbiased estimators that are based on the measurements in Equation (1). Since our main purpose is to consider the bound on the NLS estimator, we call it the CRLB for the NLS estimator in this study.

and

$$\mathbf{p}_r = \begin{bmatrix} z_r^2 - z_1^2 - k_r + k_1 \\ \vdots \\ z_r^2 - z_{r-1}^2 - k_r + k_{r-1} \\ \vdots \\ z_r^2 - z_{r+1}^2 - k_r + k_{r+1} \\ \vdots \\ z_r^2 - z_N^2 - k_r + k_N \end{bmatrix} \tag{11}$$

with

$$k_i = x_i^2 + y_i^2 \tag{12}$$

for $i = 1, 2, \ldots, N$. Note that $\mathbf{A}_r$ is an $(N-1) \times 2$ matrix that is specified by the positions of the FTs, and $\mathbf{p}_r$ is a vector of size $(N-1)$ that depends on both the FT positions and the distance measurements.

Since Equation (9) defines a linear relation, the position estimate can be obtained as [27]

$$\hat{\boldsymbol{l}}_r = (\mathbf{A}_r^{\mathrm{T}} \mathbf{A}_r)^{-1} \mathbf{A}_r^{\mathrm{T}} \mathbf{p}_r \tag{13}$$

which is the LLS estimator when the rth FT is considered as the reference FT.

Comparison of Equations (3) and (13) reveals that the LLS estimator provides a low complexity solution for position estimation. However, it also sacrifices certain amount of optimality compared to the NLS solution. This is because the LLS approach uses the measurements z_i's only through the $z_r^2 - z_i^2$ terms, for $i = 1, \ldots, r-1, r+1, N$, which causes some loss in the information contained in the set $z_1, \ldots, z_N$.

In addition to the LLS algorithm specified by Equations (10)–(13), call it *LLS-1*, there are also other versions of the LLS approach proposed in References [14–16]. The LLS estimator studied in References [14] and [15], call it *LLS-2*, subtracts each equation in Equation (8) from all the other equations, resulting in $\binom{N}{2}$ distinct linear equations. Then, the position estimate can be obtained similarly to the solution in Equation (13) for *LLS-1*. Instead of subtracting each equation from all the remaining ones, the LLS approach in References [16], call it *LLS-3*, first calculates the average of the measurements in Equation (8), and then subtracts that average from all the equations, yielding N linear relations. Again, the position estimate is obtained by the LLS solution as in Equation (13).

Similar to the *LLS-1* algorithm, the *LLS-2* and *LLS-3* algorithms also result in suboptimal position estimates compared to the NLS algorithm in Section 2, since they do not utilize all the information in the measurement set $z_1, \ldots, z_N$. In order to quantify the amount of optimality loss induced by the LLS approach, one can compare the CRLBs related to the NLS and LLS approaches.

3.2. CRLB analysis

In this section, the aim is to obtain the CRLBs for the LLS estimators described in Section 3.1. In this way, the theoretical performance difference between the NLS and LLS approaches can be comprehended *via* the comparison of the corresponding CRLB expressions. It should be noted that the NLS estimator is the ML solution under the conditions stated in Section 2; hence, it can perform very closely to the CRLB at reasonably small noise levels. However, the LLS estimators described in the previous section are not the ML solutions given the set of measurements that they are utilizing. For example, it can be shown that the *LLS-1* estimator is not the ML estimator based on $z_r^2 - z_i^2$, for $i = 1, \ldots, r-1, r+1, N$. Therefore, the LLS estimators are not guaranteed to perform very closely to the CRLBs. Hence, the difference between the CRLBs for the NLS and LLS estimators may not always provide an accurate measure of the performance improvement that would be obtained by using the NLS approach instead of one of the LLS estimators in Section 3.1.[¶] In order to compare the exact performance of the LS estimators with the CRLBs, simulation results are provided in Section 5. In addition, various LLS algorithms are proposed in Section 4, which perform more closely to the CRLB than the conventional LLS estimators in References [14–16]; hence, comparison of the CRLBs becomes more meaningful for the NLS estimators and the proposed algorithms.

In order to derive the CRLBs for the LLS estimators, the *LLS-1* estimator is considered first. Since the *LLS-1* estimator utilizes the measurements $z_i, i = 1, \ldots, N$, only through the terms $z_r^2 - z_i^2$, for $i = 1, \ldots, r-1, r+1, N$ (*cf.* Equations (9)–(13)), where r is the index of the reference FT, its measurement set is specified as

$$\tilde{z}_i = z_r^2 - z_{\tilde{i}}^2, \quad i = 1, \ldots, N-1 \tag{14}$$

where

$$\tilde{i} \doteq \begin{cases} i, & i < r \\ i+1, & i \geq r \end{cases} \tag{15}$$

In order to simplify the notation, let $r = N$ without loss of generality and $\tilde{\mathbf{z}}$ represent a vector that consists of $\tilde{z}_i$'s in Equation (14), $\tilde{\mathbf{z}} = \begin{bmatrix} z_N^2 - z_1^2 & z_N^2 - z_2^2 & \cdots & z_N^2 - z_{N-1}^2 \end{bmatrix}$.

The CRLB for any unbiased estimator that employs the measurement set $\tilde{\mathbf{z}}$ can be calculated from the conditional PDF of $\tilde{\mathbf{z}}$ given the MT position $\boldsymbol{l} = [x\ y]^{\mathrm{T}}$. From Equations (1), (2) and (14), $\tilde{z}_i = z_r^2 - z_{\tilde{i}}^2$ can be expressed, for $i = 1, \ldots, N-1$, as

$$\tilde{z}_i = k_N - k_{\tilde{i}} + 2(x_{\tilde{i}} - x_N)x + 2(y_{\tilde{i}} - y_N)y + 2n_N f_N(x, y) - 2n_{\tilde{i}} f_{\tilde{i}}(x, y) + (n_N^2 - n_{\tilde{i}}^2) \tag{16}$$

[¶] In Section 4, various approaches, including a linear ML approach, are proposed in order to narrow the gap between the performance of the LLS algorithms and the CRLBs.

where $f_i(x, y)$ and k_i are given by Equations (2) and (12), respectively. It is noted from Equation (16) that $\tilde{z}_i|\boldsymbol{l}$ can be accurately approximated by a Gaussian distribution when the noise variances are considerably smaller than the distances between the MT and the FTs, which commonly holds especially in LOS scenarios. Therefore, in order to simplify the analysis and obtain a tractable CRLB expression, the last term in Equation (16), namely $n_N^2 - n_i^2$, is modeled as a Gaussian random variable. In that case, $\tilde{z}_i$ given the MT position, that is, $\tilde{z}_i|\boldsymbol{l}$, becomes Gaussian distributed when the noise components are modeled as independent zero-mean Gaussian random variables. Under this Gaussian assumption, the conditional PDF of $\tilde{z}_i$ given $\boldsymbol{l} = [x\ y]^{\mathrm{T}}$ can be obtained, after some manipulation, as

$$\tilde{z}_i \,|\, \boldsymbol{l} \sim \mathcal{N}\Big(\mu_i(x, y), \tilde{\sigma}_i(x, y)\Big) \tag{17}$$

where

$$\mu_i(x, y) = f_N^2(x, y) - f_i^2(x, y) + \sigma_N^2 - \sigma_i^2 \tag{18}$$

$$\tilde{\sigma}_i(x, y) = 4\left[\sigma_N^2 f_N^2(x, y) + \sigma_i^2 f_i^2(x, y)\right] + 2\left(\sigma_N^4 + \sigma_i^4\right) \tag{19}$$

Also, the covariance terms can be calculated as

$$\mathrm{E}\left\{(\tilde{z}_i - \mu_i(x, y))(\tilde{z}_j - \mu_j(x, y))\right\} = 4\sigma_N^2 f_N^2(x, y) + 2\sigma_N^4 \tag{20}$$

for $i \neq j$. From Equations (17) to (20), the conditional distribution of $\tilde{\mathbf{z}}$ given $\boldsymbol{l}$ can be expressed as

$$\tilde{\mathbf{z}} \,|\, \boldsymbol{l} \sim \mathcal{N}\Big(\boldsymbol{\mu}(x, y), \boldsymbol{\Sigma}(x, y)\Big) \tag{21}$$

with $\boldsymbol{\mu}(x, y) = [\mu_1(x, y \quad \mu_2(x, y) \cdots \mu_{N-1}(x, y)]^{\mathrm{T}}$, where $\mu_i(x, y)$ is as in Equation (18) for $i = 1, \ldots, N-1$, and

$$\boldsymbol{\Sigma}(x, y) = \left(4\sigma_N^2 f_N^2(x, y) + 2\sigma_N^4\right)\mathbf{1}_{N-1} + 2\mathrm{diag}\left\{2\sigma_1^2 f_1^2(x, y) + \sigma_1^4, \ldots, 2\sigma_{N-1}^2 f_{N-1}^2(x, y) + \sigma_{N-1}^4\right\} \tag{22}$$

where $\mathbf{1}_{N-1}$ denotes an $(N-1) \times (N-1)$ matrix of ones, and $\mathrm{diag}\{a_1, \ldots, a_M\}$ represents an $M \times M$ diagonal matrix with a_i being the ith diagonal. Based on the signal model specified by Equations (21)–(22), the CRLB can be obtained as stated in the following proposition.

Proposition 1. *The CRLB on the MSE of an unbiased position estimator $\hat{\boldsymbol{l}}$ based on the measurements model in Equation (21) is given by*

$$\mathrm{E}\{\|\hat{\boldsymbol{l}} - \boldsymbol{l}\|^2\} \geq \frac{\tilde{\mathrm{I}}_{11} + \tilde{\mathrm{I}}_{22}}{\tilde{\mathrm{I}}_{11}\tilde{\mathrm{I}}_{22} - \tilde{\mathrm{I}}_{12}^2} \tag{23}$$

where[#]

$$\tilde{\mathrm{I}}_{11} = \frac{(N-1)}{2g^2}\left[g\frac{\partial^2 g}{\partial x^2} - \left(\frac{\partial g}{\partial x}\right)^2\right] + 4\mathbf{b}_x^{\mathrm{T}}\boldsymbol{\Sigma}^{-1}\mathbf{b}_x + 2\sigma_N^2 f_N^2 \sum_{i,j=1}^{N-1}\frac{\partial^2 h_{ij}}{\partial x^2} + 2\sum_{i=1}^{N-1}\sigma_i^2 f_i^2 \frac{\partial^2 h_{ii}}{\partial x^2} \tag{24}$$

$$\tilde{\mathrm{I}}_{22} = \frac{(N-1)}{2g^2}\left[g\frac{\partial^2 g}{\partial y^2} - \left(\frac{\partial g}{\partial y}\right)^2\right] + 4\mathbf{b}_y^{\mathrm{T}}\boldsymbol{\Sigma}^{-1}\mathbf{b}_y + 2\sigma_N^2 f_N^2 \sum_{i,j=1}^{N-1}\frac{\partial^2 h_{ij}}{\partial y^2} + 2\sum_{i=1}^{N-1}\sigma_i^2 f_i^2 \frac{\partial^2 h_{ii}}{\partial y^2} \tag{25}$$

$$\tilde{\mathrm{I}}_{12} = \frac{(N-1)}{2g^2}\left[g\frac{\partial^2 g}{\partial x \partial y} - \frac{\partial g}{\partial x}\frac{\partial g}{\partial y}\right] + 4\mathbf{b}_x^{\mathrm{T}}\boldsymbol{\Sigma}^{-1}\mathbf{b}_y + 2\sigma_N^2 f_N^2 \sum_{i,j=1}^{N-1}\frac{\partial^2 h_{ij}}{\partial x \partial y} + 2\sum_{i=1}^{N-1}\sigma_i^2 f_i^2 \frac{\partial^2 h_{ii}}{\partial x \partial y} \tag{26}$$

with $\boldsymbol{\Sigma}(x, y)$ *being given by Equation (22),* $g(x, y) \doteq \left|\boldsymbol{\Sigma}(x, y)\right|$, $h_{ij}(x, y) \doteq \left[\boldsymbol{\Sigma}^{-1}(x, y)\right]_{ij}$, $\mathbf{b}_x \doteq [x_1 - x_N \cdots x_{N-1} - x_N]^{\mathrm{T}}$ *and* $\mathbf{b}_y \doteq [y_1 - y_N \cdots y_{N-1} - y_N]^{\mathrm{T}}$.

Proof. Please see Appendix A. ■

Note that Proposition 1 provides generic CRLB expressions that are valid for any system configuration. Although the expressions in Equations (24)–(26) can be difficult to evaluate analytically for a large number of FTs, they still facilitate simple evaluations *via* computer programs, as employed in Section 5.

After deriving the CRLB for the *LLS-1* estimator[**] as in Proposition 1, the CRLB for *LLS-2* is considered next. Since the *LLS-2* estimator subtracts each equation in Equation (8) from all the other equations, it utilizes the measurements z_i, for $i = 1, \ldots, N$, only through the following terms:

$$\check{z}_{ij} = z_i^2 - z_j^2, \qquad i, j = 1, 2, \ldots, N,\ i < j \tag{27}$$

[#] The function arguments (x, y)'s are omitted in order to have simpler expressions.

[**] It should be noted that 'the CRLB for the *LLS-1* estimator' more generally means 'the CRLB for any unbiased estimator based on the linearized measurements in Equation (14)'.

Note that *LLS-2* employs more measurements than *LLS-1* (*cf*. Equation (14)). However, it is observed that all the additional measurements in Equation (27) can be obtained from the differences of the measurements in Equation (14). In other words, there are no independent measurements, or additional information, in the measurement set for the *LLS-2* algorithm compared to *LLS-1*. Therefore, the CRLB expression for the *LLS-1* estimator is also valid for *LLS-2*.

Finally, the CRLB for the *LLS-3* estimator is considered. Since *LLS-3* subtracts the average of the measurements in Equation (8) from all the equations, it effectively utilizes the following measurements set:

$$\bar{z}_i = z_i^2 - \frac{1}{N}\sum_{j=1}^{N} z_j^2, \qquad i = 1, 2, \ldots, N \tag{28}$$

Although this measurements set seems to be quite different from that in Equation (14) for the *LLS-1* estimator, the following proposition states that it carries the same amount of statistical information as the one in Equation (14).

Proposition 2. *The CRLB for estimating the MT position based on the measurements set in Equation (28) is the same as the CRLB based on the measurements set in Equation (14).*

Proof. Please see Appendix B. ■

After obtaining the CRLB expression for the LLS algorithms, the aim is to improve the performance of those algorithms and make them perform closely to the CRLB.

4. REFERENCE FT SELECTION AND ML ESTIMATION FOR LOS AND NLOS SCENARIOS

In this section, two approaches, namely, reference selection and ML estimation, are proposed in order to improve the performance of the LLS estimators. Although the algorithms are developed for the *LLS-1* technique in the following, the proposed ML approach can also be applied to the *LLS-2* and *LLS-3* techniques in a similar manner.

To develop the framework of the proposed algorithms, the vector $\mathbf{p}_r$ in Equation (11) is expanded as follows:

$$\mathbf{p}_r = \mathbf{p}_r^{(c)} + \mathbf{p}_r^{(n)} \tag{29}$$

where $\mathbf{p}_r^{(c)}$ and $\mathbf{p}_r^{(n)}$ denote the constant and the noisy components of $\mathbf{p}_r$, respectively [28]. From Equations (1) and (11), $\mathbf{p}_r^{(c)}$ and $\mathbf{p}_r^{(n)}$ can be expressed as

$$\mathbf{p}_r^{(c)} = \begin{bmatrix} f_r^2(x,y) - f_1^2(x,y) - k_r + k_1 \\ \vdots \\ f_r^2(x,y) - f_{r-1}^2(x,y) - k_r + k_{r-1} \\ f_r^2(x,y) - f_{r+1}^2(x,y) - k_r + k_{r+1} \\ \vdots \\ f_r^2(x,y) - f_N^2(x,y) - k_r + k_N \end{bmatrix}$$

$$\mathbf{p}_r^{(n)} = \begin{bmatrix} 2f_r(x,y)n_r - 2f_1(x,y)n_1 + n_r^2 - n_1^2 \\ \vdots \\ 2f_r(x,y)n_r - 2f_{r-1}(x,y)n_{r-1} + n_r^2 - n_{r-1}^2 \\ 2f_r(x,y)n_r - 2f_{r+1}(x,y)n_{r+1} + n_r^2 - n_{r+1}^2 \\ \vdots \\ 2f_r(x,y)n_r - 2f_N(x,y)n_N + n_r^2 - n_N^2 \end{bmatrix} \tag{30}$$

4.1. Reference FT selection for LOS scenarios

The *LLS-1* estimator studied in Section 3 arbitrarily selects one of the FTs as the reference. However, observation of the noisy terms in $\mathbf{p}_r^{(n)}$ (*cf*. Equation (30)) reveals that *all* the rows of the vector $\mathbf{p}_r^{(n)}$ depend on the true distance between the MT and the reference FT, i.e., $f_r(x, y)$, and the noise component related to that reference, i.e., n_r. For example, if the reference FT is away from the MT, this implies that all the elements of vector $\mathbf{p}_r$ can include larger noise terms, degrading the position estimation accuracy. Therefore, selection of the reference FT may considerably affect the MSE of the estimator.

In order to develop an optimal selection strategy, first express the estimator in Equation (13) as follows:

$$\hat{l}_r = \mathbf{B}_r\mathbf{p}_r^{(c)} + \mathbf{B}_r\mathbf{p}_r^{(n)} \tag{31}$$

where $\mathbf{B}_r \doteq (\mathbf{A}_r^{\mathrm{T}}\mathbf{A}_r)^{-1}\mathbf{A}_r^{\mathrm{T}}$, and $\mathbf{p}_r^{(c)}$ and $\mathbf{p}_r^{(n)}$ are given by Equation (30). Since the second term on the right-hand-side of Equation (31) is due to noise, the 'best' reference FT can be selected as the one that minimizes the expected value of the square of the L_2-norm for that term; i.e.,

$$r_{\mathrm{opt}} = \arg \min_{r\in\{1,\ldots,N\}} \mathrm{E}\left\{ \left|\left| \mathbf{B}_r\mathbf{p}_r^{(n)} \right|\right|_2^2 \right\} \tag{32}$$

If the elements of $\mathbf{B}_r$ are denoted as

$$\mathbf{B}_r \doteq \begin{bmatrix} \eta_{r,1} & \cdots & \eta_{r,r-1} & \eta_{r,r+1} & \cdots & \eta_{r,N} \\ \upsilon_{r,1} & \cdots & \upsilon_{r,r-1} & \upsilon_{r,r+1} & \cdots & \upsilon_{r,N} \end{bmatrix} \quad (33)$$

the expectation in Equation (32) can be obtained from Equation (30) as

$$\mathrm{E}\left\{ \left|\left| \mathbf{B}_r \mathbf{p}_r^{(\mathrm{n})} \right|\right|_2^2 \right\} = \sum_{\substack{i=1 \\ i\neq r}}^{N} \sum_{\substack{j=1 \\ j\neq r}}^{N} \eta_{r,i}\eta_{r,j}\, \mathrm{E}\{F_{r,i}F_{r,j}\} + \sum_{\substack{i=1 \\ i\neq r}}^{N} \sum_{\substack{j=1 \\ j\neq r}}^{N} \upsilon_{r,i}\upsilon_{r,j}\, \mathrm{E}\{F_{r,i}F_{r,j}\} \quad (34)$$

where[††]

$$F_{r,i} \doteq 2 f_r(x, y) n_r + n_r^2 - 2 f_i(x, y) n_i - n_i^2 \quad (35)$$

As the noise components are distributed as $n_i \sim \mathcal{N}(0, \sigma_i^2)$ in the LOS case, $\mathrm{E}\{F_{r,i}F_{r,j}\}$ in Equation (34) can be calculated, after some manipulation, as

$$\mathrm{E}\{F_{r,i}F_{r,j}\} = 4 f_r^2(x, y)\sigma_r^2 + 3\sigma_r^4 - \sigma_r^2(\sigma_i^2 + \sigma_j^2) + I_{i,j} \quad (36)$$

where

$$I_{i,j} = \begin{cases} \sigma_i^2\sigma_j^2, & i \neq j \\ 4 f_i^2(x, y)\sigma_i^2 + 3\sigma_i^4, & i = j \end{cases} \quad (37)$$

From Equations (34), (36), and (37), the optimal reference FT can be determined *via* Equation (32). Note that the exact solution of the optimization problem requires the knowledge of the $f_i(x, y)$ terms, which are not available in practice. Therefore, the noisy measurements z_i can be used as their estimates in the calculations. Once the reference FT is selected through Equation (32), the matrix $\mathbf{A}_r$ in Equation (10) and the vector $\mathbf{p}_r$ in Equation (11) can be obtained using this selected reference FT (FT-r_{opt}), and the position estimate is then obtained from Equation (13). The resulting estimator is referred as *LLS* with reference selection (*LLS-RS*).

In the case of equal noise variances, i.e., $\sigma_i^2 = \sigma^2\ \forall\, i$, it can be shown that Equation (32) is minimized by selecting the reference FT as the one that has the minimum (measured) distance, i.e.,[‡‡]

$$r_{\mathrm{opt}} = \arg \min_{i\in\{1,\ldots,N\}} \{z_i\} \quad (38)$$

[††]The argument (x, y) is omitted for the function $F_{r,i}$ for simplicity of notation.

[‡‡]Again the measurement z_i is used as an estimate of the true distance $f_i(x, y)$.

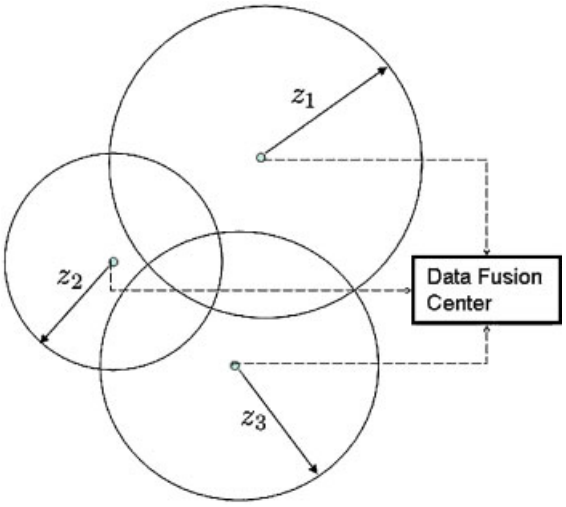

Figure 1. Trilateration yields multiple intersection of circles defined by TOA measurements in the presence of noise.

For example, in Figure 1, FT-2 is used to obtain the linear model from nonlinear expressions (i.e., selected as the reference), since z_2 is the minimum among all the measured distances. Note that even for different noise variances, if the FT having the smallest measured distance also has the smallest noise variance (which is typically the case), Equation (38) still minimizes the expectation in Equation (32); hence, it is a practical simplification for typical scenarios.

4.2. Reference FT selection for NLOS scenarios

In NLOS scenarios, it is more complicated to select an optimal reference FT due to the presence of NLOS errors. Specifically, the noise components are no longer zero mean Gaussian random variables in NLOS scenarios, and the statistical information about the noise components can be limited. Depending on the amount of *a-priori* information about the NLOS noise, various approaches can be considered for optimal reference FT selection.

4.2.1. Case-1: NLOS bias estimates are available.

In some cases, noise in NLOS measurements can be modeled as the summation of a constant NLOS bias and a zero mean Gaussian error. If an estimate of the NLOS bias is obtained (e.g., as in Reference [13]), then the measurements can be corrected by that estimate, and the LOS reference selection rule in Equation (32) can be employed. However, estimation of NLOS biases is typically quite challenging.

4.2.2. Case-2: Identities of NLOS FTs are available.

If the knowledge of which FTs are in NLOS of the MT is available (but NLOS noise statistics are unavailable), then a simple reference selection technique utilizing the minimum distance measurement criteria and only the LOS FTs can be stated as follows (call it *LLS-RS-LO*)[§§]

$$r_{\text{opt}} = \arg \min_{i \in \mathcal{C}_{\text{LOS}}} \{z_i\} \tag{39}$$

where $\mathcal{C}_{\text{LOS}}$ denotes the index set for all the LOS FTs. Some NLOS identification techniques as in References [22--24,29] can be used to determine the NLOS FTs and exclude them from the set $\mathcal{C}_{\text{LOS}}$. Note that the geometry of the terminals and how the reference FT is placed with respect to the NLOS FTs and the MT become more important in an NLOS scenario. A drawback of Equation (39) is that it never selects an NLOS FT as the reference. However, in the cases of small NLOS errors, it may be preferable to select an NLOS FT as the reference if it is sufficiently close to the MT.

4.2.3. Case-3: NLOS noise statistics are available.

Now consider that the following statistical information is available about the NLOS noise related to the ith reference FT:

$$\text{E}\{n_i\} = \mu_i,\ \text{E}\{n_i^2\} = \mu_{2,i},\ \text{E}\{n_i^3\} = \mu_{3,i},\ \text{E}\{n_i^4\} = \mu_{4,i} \tag{40}$$

Then, the optimal reference FT can be selected according to the optimality criterion in Equation (32). In that case, the cost function in Equation (34) should be calculated based on the available NLOS statistics:

$$\text{E}\{F_{r,i}F_{r,j}\} = \begin{cases} H_r + H_i - 2G_iG_r, & i = j \\ H_r + G_iG_j - G_r(G_i + G_j), & i \neq j \end{cases} \tag{41}$$

where

$$H_i = 4f_i^2(x, y)\mu_{2,i} + 4f_i(x, y)\mu_{3,i} + \mu_{4,i} \tag{42}$$

$$G_i = 2f_i(x, y)\mu_i + \mu_{2,i} \tag{43}$$

Since the true distances $f_i(x, y)$ are not available in practice, the unbiased estimates $z_i - \mu_i$ are used instead of $f_i(x, y)$ in evaluating Equations (41)–(43). Also, it is observed that Equations (41)–(43) reduce to Equations (36) and (37) for LOS scenarios, for which

$$\mu_i = \mu_{3,i} = 0,\ \mu_{2,i} = \sigma_i^2,\ \mu_{4,i} = 3\sigma_i^4 \tag{44}$$

Note that when the noise moments are specified as in Equation (40), it is more practical to modify the NLS algorithm as in Equation (4) by subtracting the noise means from the measurements. Therefore, the effective noise in the measurements that are employed in the LLS estimation can be described by the $\xi_i \doteq n_i - \mu_i$ terms. Hence, the moments in Equation (40) become

$$\text{E}\{\xi_i\} = 0,\ \text{E}\{\xi_i^2\} = \sigma_i^2,\ \text{E}\{\xi_i^3\} = \breve{\mu}_{3,i},\ \text{E}\{\xi_i^4\} = \breve{\mu}_{4,i} \tag{45}$$

and Equation (41) can be evaluated for $H_i = 4f_i^2(x, y)\sigma_i^2 + 4f_i(x, y)\breve{\mu}_{3,i} + \breve{\mu}_{4,i}$ and $G_i = \sigma_i^2$.

4.3. ML estimation for LOS scenarios

As discussed in Section 3.2, the LLS estimators may not perform very closely to the CRLBs since they are not the ML solutions for the considered measurements sets. Specifically, the LLS approach does not take into account the correlations between the rows of the vector $\mathbf{p}_r^{(\text{n})}$, which become correlated due to the linearization process. In this section, an improved LLS technique is proposed based on the ML approach which naturally takes the correlations in the measurements into account.

In order to derive the ML estimator in the presence of correlated measurements [30], the expression in Equation (29) can be reformulated, by using $\mathbf{p}_r^{(\text{c})} = \mathbf{A}_r\boldsymbol{l}$ with $\boldsymbol{l}$ being the true location of the MT, as

$$\mathbf{p}_r = \mathbf{A}_r\boldsymbol{l} + \mathbf{p}_r^{(\text{n})} \tag{46}$$

In order to obtain an estimator with low computational complexity, it is assumed that $\mathbf{p}_r^{(\text{n})}$ can be modeled as a jointly Gaussian random vector as in Section 3. Note from Equation (30) that when the noise terms are small compared to the distances between the FTs and the MT, the assumption becomes more accurate. If the distribution of $\mathbf{p}_r^{(\text{n})}$ is represented by $\mathbf{p}_r^{(\text{n})} \sim \mathcal{N}(\boldsymbol{\mu}_r, \mathbf{C}_r)$, the conditional PDF of $\mathbf{p}_r$ in Equation (46) given $\boldsymbol{l}$ can be expressed as $\mathbf{p}_r|\,\boldsymbol{l} \sim \mathcal{N}(\mathbf{A}_r\boldsymbol{l} + \boldsymbol{\mu}_r, \mathbf{C}_r)$. Then, the ML solution is given by [30]

$$\hat{\boldsymbol{l}}_r = \arg\min_{\boldsymbol{l}} \left\{ \boldsymbol{l}^{\text{T}}\mathbf{A}_r^{\text{T}}\mathbf{C}_r^{-1}\mathbf{A}_r\boldsymbol{l} - 2(\mathbf{p}_r - \boldsymbol{\mu}_r)^{\text{T}}\mathbf{C}_r^{-1}\mathbf{A}_r\boldsymbol{l} \right\} \tag{47}$$

from which the ML estimator (MLE) can be derived as

$$\hat{\boldsymbol{l}} = (\mathbf{A}_r^{\text{T}}\mathbf{C}_r^{-1}\mathbf{A}_r)^{-1}\mathbf{A}_r^{\text{T}}\mathbf{C}_r^{-1}(\mathbf{p}_r - \boldsymbol{\mu}_r) \tag{48}$$

When all the FTs are in LOS, the mean of $\mathbf{p}_r^{(\text{n})}$ can be obtained from Equation (30) as

[§§]Here, *LLS-RS-LO* refers to the LLS estimator with **r**eference **s**election that uses the **L**OS measurements **o**nly.

$$\boldsymbol{\mu}_r = \left[\sigma_r^2-\sigma_1^2 \quad \cdots \quad \sigma_r^2-\sigma_{r-1}^2 \quad \sigma_r^2-\sigma_{r+1}^2 \quad \cdots \quad \sigma_r^2-\sigma_N^2 \right]^{\mathrm{T}} \tag{49}$$

On the other hand, it is observed from Equations (30) and (35) that the elements of the covariance matrix $\mathbf{C}_r$ of vector $\mathbf{p}_r^{(\mathrm{n})}$ can be calculated as

$$[\mathbf{C}_r]_{ij} = \mathrm{E}\{F_i F_j\} - [\boldsymbol{\mu}_r]_i [\boldsymbol{\mu}_r]_j \tag{50}$$

where $\mathrm{E}\{F_i F_j\}$ is given by Equations (36) and (37), and $[\boldsymbol{\mu}_r]_i$ is the ith element of $\boldsymbol{\mu}_r$ in Equation (49). Again note that $f_i(x, y)$ terms in the calculations should be replaced by their estimates, z_i's.

4.4. ML estimation for NLOS scenarios

The MLE in NLOS scenarios is the same as the formulation in Equation (48), when $\mathbf{C}_r$ and $\boldsymbol{\mu}_r$ are replaced by appropriate values considering NLOS noise statistics. Assuming that the statistics of the NLOS noise components are available as in Equation (40), the mean $\boldsymbol{\mu}_r$ can be expressed as

$$\boldsymbol{\mu}_r = \begin{bmatrix} 2f_r(x, y)\mu_r + \mu_{2,r} - 2f_1(x, y)\mu_1 - \mu_{2,1} \\ \vdots \\ 2f_r(x, y)\mu_r + \mu_{2,r} - 2f_{r-1}(x, y)\mu_{r-1} - \mu_{2,r-1} \\ 2f_r(x, y)\mu_r + \mu_{2,r} - 2f_{r+1}(x, y)\mu_{r+1} - \mu_{2,r+1} \\ \vdots \\ 2f_r(x, y)\mu_r + \mu_{2,r} - 2f_N(x, y)\mu_N - \mu_{2,N} \end{bmatrix} \tag{51}$$

while the covariance matrix $\mathbf{C}_r$ is calculated as in Equation (50) by using Equations (41)–(43) for the first term and Equation (51) for the second term.

4.5. Summary of improved LLS algorithms and complexity comparison

A generic block diagram for the proposed improvements over the conventional *LLS-1* estimator is illustrated in Figure 2. First, from N distance measurements, which can, for example, be obtained from TOA measurements, a reference FT is selected. Reference selection is performed according to the optimization problem defined by Equation (32). For LOS scenarios, the cost function of the optimization problem is specified by Equations (33)–(37). In addition, for equal noise variances, that is, for $\sigma_i^2 = \sigma^2 \ \forall i$, the reference selection problem simplifies to Equation (38).[|||] On the other hand, for NLOS scenarios, the reference selection rule is based on the same optimization problem in Equation (32), but the cost function is evaluated differently for various NLOS situations (*cf.* Equations (39)–(43)).

While the knowledge of noise variance is sufficient for evaluating Equation (32) in an LOS scenario, the first four moments of the noise variance are employed in order to evaluate Equation (39) in certain NLOS scenarios (Case-3 in Section 4.2). If the estimates for the NLOS biases are available, they can be subtracted from the biased measurements, followed by the LOS reference selection rule (Case-1 in Section 4.2). On the other hand, if only the indices of the NLOS FTs are available, they may simply be excluded from the set of candidate reference FTs if there are at least three LOS FT measurements (Case-2 in Section 4.2).

Once the reference FT is selected, the corresponding distance measurement is used to obtain a set of $N-1$ linear equations corresponding to the remaining FTs, and the position estimate is obtained through the LLS estimator in Equation (13). Alternatively, an $(N-1) \times (N-1)$ covariance matrix can be obtained as described in Section 4.3 or Section 4.4 for LOS or NLOS scenarios, respectively, followed by an MLE solution as in Equation (48). Although the proposed reference selection techniques are specific to the *LLS-1* estimator, the ML estimation technique, which improves position estimation by taking correlations between measurements into account, can be applied to the *LLS-2* and *LLS-3* estimators, as well.

It is useful to compare the computational complexities of the different techniques discussed in the paper for a better understanding of their applicability to low-complexity systems. Computational complexities of different methods can be obtained in terms of their CPU cycle counts by considering the individual cycle counts for addition (ADD), multiplication (MUL), and comparison (CMP) operations. For example, in a Xilinx DSP48 slice, these cycle counts are 1, 3, and 1, respectively, for ADD, MUL, and CMP operations [31]. Table I presents a breakdown of number of cycle counts required for each operation corresponding to four different LLS methods, where $N_{\mathrm{p}} = \binom{N}{2}$ and it is assumed that the noise variance at all the FTs are identical. It can easily be seen that complexity of *LLS-1*, *LLS-3*, and *LLS-RS* are $\mathcal{O}(N)$, while complexity of *LLS-2* is $\mathcal{O}(N^2)$ due to large matrix sizes of $N_{\mathrm{p}} \times N_{\mathrm{p}}$ that are involved. While it is not specifically included in Table I, complexity of *MLE* is $\mathcal{O}(N^3)$ due to the inversion of $(N-1) \times (N-1)$ covariance matrices in Equation (48). Therefore, MLE has significantly larger complexity compared to all four of the LLS techniques. In Figure 3, CPU cycle counts of different algorithms are plotted with respect to the number of FTs in the environment. The *LLS-RS* is seen to have minimal computational complexity increase compared to that of *LLS-1*, and better computational complexities compared to *LLS-2* and *LLS-3*. As will be shown in the next section, *LLS-RS* also outperforms the localization accuracies of all the other three LLS methods.

[|||] The simplified selection rule is also valid if the measurement variance increases with increasing distance as in many practical scenarios.

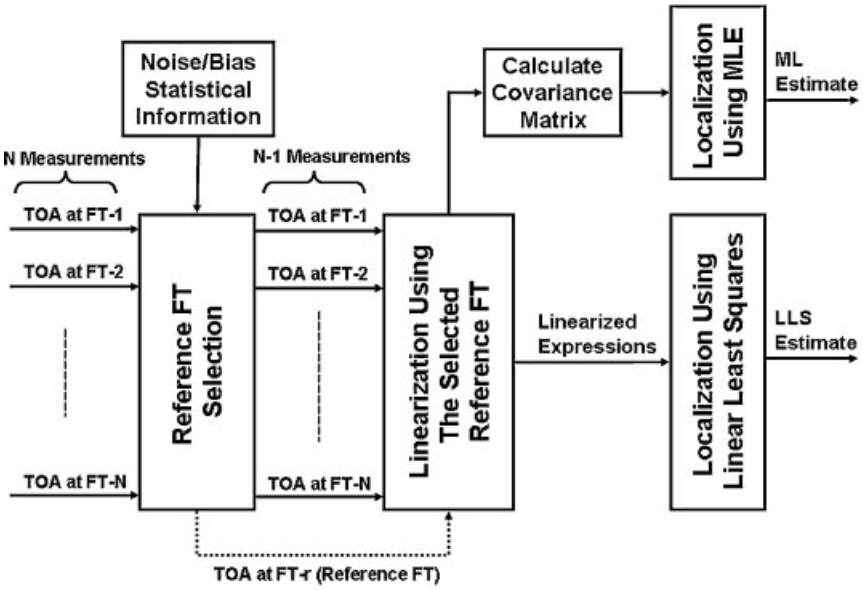

Figure 2. Block diagram of the proposed reference FT selection and MLE algorithms.

5. SIMULATION RESULTS

In this section, simulation studies are performed in order to evaluate the CRLBs and compare the performance of the LLS algorithms studied in the previous section. In the simulation environment, different numbers of FTs are considered for position estimation, as illustrated in Figure 4. In particular, we consider position estimation with 3, 4, 5, and

Table I. Number of computations required for different algorithms.

Operation	MUL	ADD	CMP
LLS-1			
Calculate $\mathbf{A}_r$	$2(N-1)$	$2(N-1)$	
Calculate $\mathbf{p}_r$	$3N$	$3(N-1)$	
Calculate $\mathbf{A}_r^{\mathrm{T}}\mathbf{p}_r$	$2(N-1)$	$2(N-2)$	
Calculate $(\mathbf{A}_r^{\mathrm{T}}\mathbf{A}_r)^{-1}$	$4N+4$	$4N-7$	
Product of $(\mathbf{A}_r^{\mathrm{T}}\mathbf{A}_r)^{-1}$ and $\mathbf{A}_r^{\mathrm{T}}\mathbf{p}_r$	4	2	
LLS-2			
Calculate $\mathbf{A}_r$	$2N_{\mathrm{p}}$	$2N_{\mathrm{p}}$	
Calculate $\mathbf{p}_r$	$3N$	$3N_{\mathrm{p}}+N$	
Calculate $\mathbf{A}_r^{\mathrm{T}}\mathbf{p}_r$	$2N_{\mathrm{p}}$	$2(N_{\mathrm{p}}-1)$	
Calculate $(\mathbf{A}_r^{\mathrm{T}}\mathbf{A}_r)^{-1}$	$4N_{\mathrm{p}}+8$	$4N_{\mathrm{p}}-3$	
Product of $(\mathbf{A}_r^{\mathrm{T}}\mathbf{A}_r)^{-1}$ and $\mathbf{A}_r^{\mathrm{T}}\mathbf{p}_r$	4	2	
LLS-3			
Calculate $\mathbf{A}_r$	$2(N+1)$	$4N$	
Calculate $\mathbf{p}_r$	$6N+3$	$8N$	
Calculate $\mathbf{A}_r^{\mathrm{T}}\mathbf{p}_r$	$2N$	$2(N-1)$	
Calculate $(\mathbf{A}_r^{\mathrm{T}}\mathbf{A}_r)^{-1}$	$4N+8$	$4N-3$	
Product of $(\mathbf{A}_r^{\mathrm{T}}\mathbf{A}_r)^{-1}$ and $\mathbf{A}_r^{\mathrm{T}}\mathbf{p}_r$	4	2	
LLS-RS			
Calculate $\arg\min_{i\in\{1,\ldots,N\}}\{z_i\}$			N
Calculate $\mathbf{A}_r$	$2(N-1)$	$2(N-1)$	
Calculate $\mathbf{p}_r$	$3N$	$3(N-1)$	
Calculate $\mathbf{A}_r^{\mathrm{T}}\mathbf{p}_r$	$2(N-1)$	$2(N-2)$	
Calculate $(\mathbf{A}_r^{\mathrm{T}}\mathbf{A}_r)^{-1}$	$4N+4$	$4N-7$	
Product of $(\mathbf{A}_r^{\mathrm{T}}\mathbf{A}_r)^{-1}$ and $\mathbf{A}_r^{\mathrm{T}}\mathbf{p}_r$	4	2	

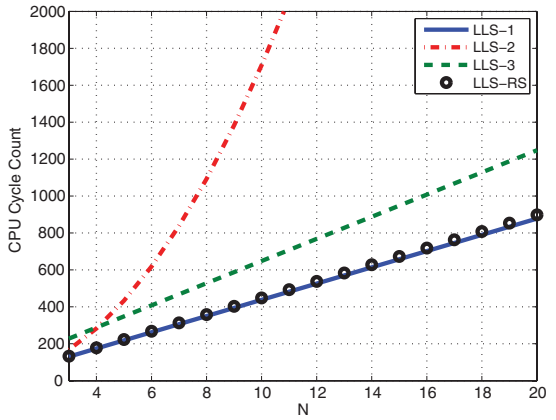

Figure 3. Comparison of computational complexities of different algorithms as a function of number of FTs.

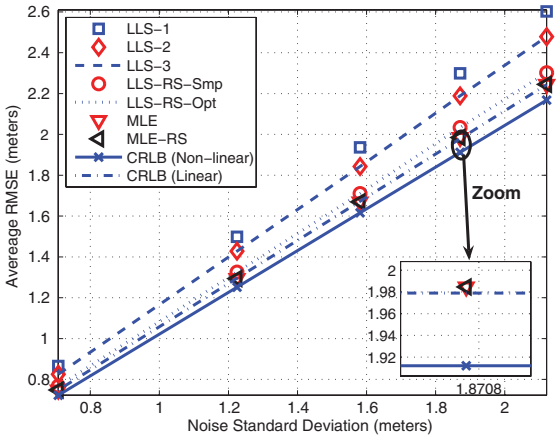

Figure 5. RMSE versus the noise variance (equal noise variances are assumed for all FTs) for the linear LS algorithms, and the CRLBs.

6 FTs, which are represented by triangles, squares, pentagrams, and hexagrams, respectively. In each case, the FTs are located with uniform spacing over a circle centered at the origin with a radius of 100 m. As illustrated in Figure 4, a grid of 15 × 15 test locations (marked by small dots) are considered and performance metrics (including the CRLBs) are calculated as the averages over those different locations. For simplicity, the same noise variances are assumed for all the distance measurements in LOS scenarios, i.e., $\sigma_i^2 = \sigma^2$.

First, an LOS scenario is considered with four FTs as in Figure 4, where the FTs are labeled as FT-1, FT-2, FT-3, and FT-4. The average root mean-squared error (RMSE) results for different algorithms and the CRLBs for this scenario are presented in Figure 5. It is observed that there is a linear relation between the standard deviation of the noise and the RMSE, which can also be observed from Equations (6) and (7) for the CRLB in the nonlinear case. Comparison of the three LLS algorithms reveals that *LLS-2* and *LLS-3* have the same performance, which is better than that of *LLS-1*. In other words, *LLS-1* has the highest RMSEs. The worst performance of *LLS-1* is mainly due to its estimation

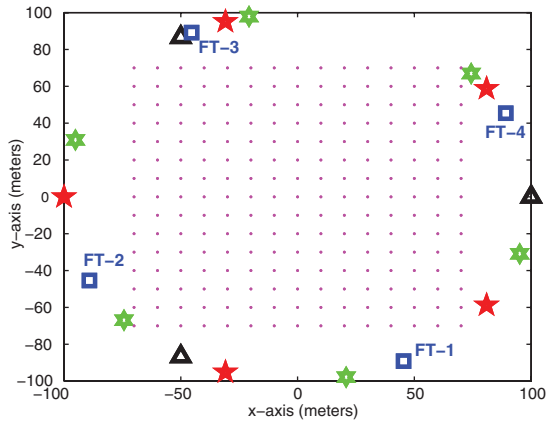

Figure 4. Simulation environment with 3, 4, 5, and 6 FTs, where the coordinates are in the unit of meters.

technique which uses one of the FTs as the reference for other measurements (*cf.* Equation (14)). In the presence of large noise in the reference, the estimate can have significant errors. However, *LLS-2* and *LLS-3* have an averaging effect in selecting the reference, since not only a single measurement is used as the reference (*cf.* Equations (27) and (28)).

Another observation from Figure 5 is that there is considerable difference between the theoretical limits, CRLBs, and the performance of the prior-art LLS algorithms. For example, for a noise standard deviation of 2 m, the performance difference between *LLS-1* and the CRLB is about 0.4 m. When the optimal RS technique described in Equation (32), call it *LLS-RS-Opt*, is used, the average localization performance approaches to the CRLB significantly, and it performs better than all the prior-art LLS algorithms. Moreover, since the noise variances are the same for different FTs in this scenario, the simplified version of the reference selection technique in Equation (38), call it *LLS-RS-Smp*, performs equally well. Some further performance gain is obtained through utilizing the MLE method in Equation (48). Also, the results show that the reference selection technique does not modify the performance of the MLE method for an LOS scenario. Finally, the CRLBs for the linear and nonlinear cases in Section 2 and Section 3, respectively, seem to have close values, but the CRLB for the nonlinear case is lower than that for the linear case, as expected. Also, the proposed techniques, especially the ML approach, narrow the gap between the performance of linear position estimation and the CRLB significantly.

The topology and the number of FTs can have significant impacts on positioning accuracy. In order to observe how the RMSEs change for different numbers of FTs, simulation results are obtained for scenarios with 3, 4, 5, and 6 FTs in Figure 4. Since the RMSE of a certain algorithm has a linear relation with the standard deviation of noise for LOS scenarios, the following metric is employed [1], $\text{GDOP}_{\text{avg}} = \frac{\text{Average RMSE}}{\sigma}$, which is referred to as the

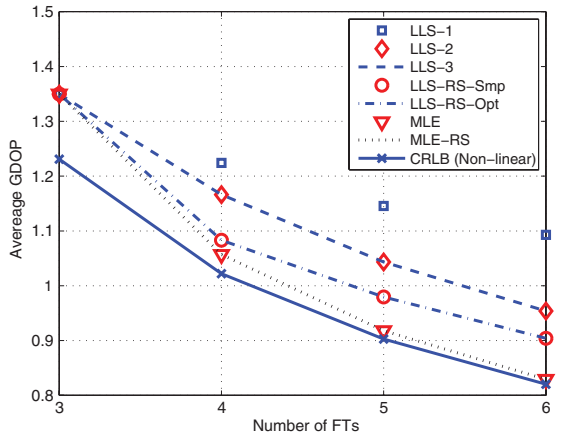

Figure 6. Average GDOP versus the number of FTs for various algorithms.

average geometric dilution of precision (GDOP), and is independent of the noise standard deviation. In Figure 6, the average GDOPs are plotted versus the number of FTs involved in position estimation for various algorithms. The results indicate that when there is a larger number of FTs, the performance gap between *LLS-1* and *LLS-RS* increases, and it becomes more advantageous to use the *LLS-RS* algorithm. This is because at a particular test location, it becomes more likely to find a better FT for linearization purposes. Another critical observation is that the MLE converges to the CRLB as the number FTs increases. Moreover, as the number of FTs increases, average GDOP value becomes less than one. Based on the definition of GDOP, this implies that the variance of the position estimate becomes smaller than the variance of the individual distance measurements for large N.

For NLOS simulations, we consider the topology with 4 FTs as in Figure 4, and FT-4 is taken as the NLOS FT (the remaining FTs are all in LOS of the MT). In Figure 7, the simulation results for *LLS-1* are presented for $\sigma^2 \in \{0.3, 3\}\,\mathrm{m}^2$ when different FTs are selected as the reference

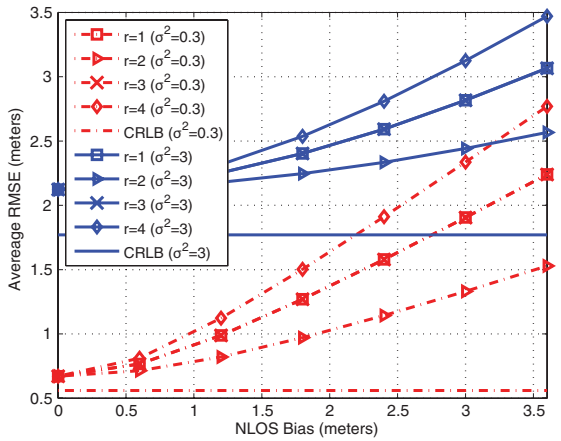

Figure 7. Performance of *LLS-1* for various NLOS scenarios.

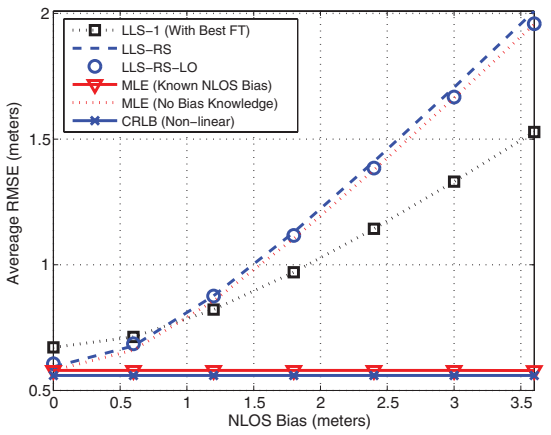

Figure 8. Average RMSE versus NLOS bias ($\sigma^2 = 0.3\,\mathrm{m}^2$).

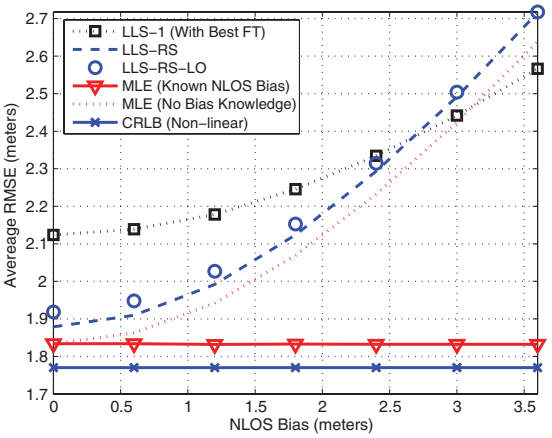

Figure 9. Average RMSE versus NLOS bias ($\sigma^2 = 3\,\mathrm{m}^2$).

FT[¶¶]. The NLOS noise at FT-4 is modeled as the sum of a constant bias b_4 and the Gaussian measurement noise as in LOS measurements. The NLOS bias at FT-4 is changed from 0 to 3.6 m. The CRLBs with biased measurements are also indicated. A critical observation is that when FT-4 is selected as the reference FT (i.e., when $r = 4$), the average RMSEs become the largest for all scenarios. This verifies the claim that on the average, an NLOS FT should not be selected as the reference FT[***]. On the other hand, FT-2, which is the FT that is the furthest from the NLOS FT[†††], is the best reference FT to select for both $\sigma^2 = 0.3\,\mathrm{m}^2$ and $\sigma^2 = 3\,\mathrm{m}^2$.

[¶¶]The RMSE of LLS-1 has been derived in closed form in the presence of NLOS bias in References [18,19]. However, comparison of different selections of the reference FT has not been performed.

[***]The RMSEs are averaged over different locations on the grid, and given b_4, there may be individual locations close to FT-4 on the grid where selecting FT-4 as the reference may be preferable.

[†††]As an alternative method to *LLS-RS*, the reference FT can be selected and fixed for a given set of user locations, which may be an efficient approach if users are clustered around certain regions.

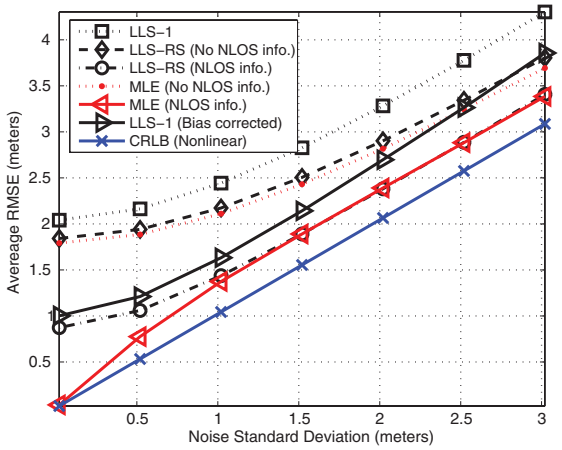

Figure 10. Average RMSE versus noise standard deviation when FT-4 is subject to an additional NLOS noise with mean 3 m and variance 3 m^2.

The NLOS simulations in Figures 8 and 9 compare the accuracies of the proposed techniques with those of *LLS-1* for different values of σ^2. FT-2 (which is the best reference FT on the average according to Figure 7) is always selected as the reference FT for *LLS-1*. Again, the NLOS noise is modeled as the sum of a constant bias and the Gaussian measurement noise as in LOS measurements. The results show that *LLS-RS* and *LLS-RS-LO* perform better than *LLS-1* for LOS scenarios or for small NLOS bias values. When the NLOS bias value gets larger, after some point, *LLS-1* starts performing better. This is because *LLS-RS* uses the measured distances, which gets considerably biased as the NLOS bias increases. For larger σ^2, the range of the NLOS bias values where *LLS-RS* beats *LLS-1* gets larger. Moreover, it is observed that there is only marginal improvement of using *LLS-RS-LO* rather than *LLS-RS*, which appears when σ^2 is small and when the NLOS bias is large. This is because *LLS-RS-LO* never selects the NLOS FT as the reference FT even when the MT is very close to it. In both figures, the MLE with perfect bias knowledge performs close to the CRLB (as in an LOS scenario)[‡‡‡], while without any knowledge of the NLOS bias, it still performs better than *LLS-RS*.

Finally, in Figure 10, performances of various algorithms are compared for the four FT scenarios in Figure 4, when the FT-4 is subject to an additional Gaussian NLOS noise with a mean of 3 m and a variance of 3 $meters^2$. All the FTs are also subject to measurement noise with a standard deviation indicated on the x-axis of Figure 10. The results indicate that the *LLS-1* estimator, which uses the measurements without any bias adjustment as in Equation (4) and selects FT-1 as the reference FT, has the worst performance among all the algorithms. For comparison purposes, the results for the LLS-RS and MLE algorithms that do not have any information about the NLOS noise statistics are also plotted ('*LLS-RS* (No NLOS info.)' and 'MLE (No NLOS info.)', respectively). When the statistics of the NLOS noise is known, a reasonable approach for least-squares algorithms is to subtract the mean of the NLOS noise from the related measurement as shown in Equation (4). When the *LLS-1* estimator is implemented based on such bias corrected measurements, its performance can increase significantly as shown by the '*LLS-1* (Bias corrected)' curve in Figure 10. It is observed that the performance of the bias corrected *LLS-1* estimator can still be improved *via* the proposed reference selection and ML approaches by using the statistical information about the NLOS noise. The curves 'LLS-RS (NLOS info.)' and 'MLE (NLOS info.)' refer to position estimation based on the proposed approaches in Section 4.2 and Section 4.4, respectively. The resulting estimators perform more closely to the CRLB, and specifically, the MLE algorithm performs better than all the algorithms especially at low measurement noise levels.

[‡‡‡] One can also consider *LLS-RS* with perfect bias knowledge, which would yield the same accuracy as in an LOS scenario.

6. CONCLUDING REMARKS

While location estimation based on non-linear observations provides high localization accuracy, it has large computational complexities. Using linearized observations allows significant reduction in the computational complexity. In this paper, a generic CRLB expression has been derived for position estimators that utilize linearized measurements. This CRLB expression quantifies the performance loss in using linearized measurements in least-squares estimators. In order to reduce that performance loss, both reference selection and ML techniques have been proposed. In reference selection, the reference FT is selected optimally according to the cost function in Equation (32). In addition, the ML technique takes into account the correlations between linear measurements and provides further performance improvement. Computational complexities of different approaches have also been compared. Simulation results indicate that both techniques perform better than the prior-art LLS estimators and reduce the gap between theoretical limits and practical algorithms. Proposed low-complexity techniques with good localization accuracy may be useful, for example, for wireless sensor network applications, which require low computational complexity due to battery/hardware limitations.

APPENDIX A

Proof of Proposition 1. From Equation (21) to (22), the log-likelihood function of $\tilde{\mathbf{z}}$ given $\boldsymbol{l} = [x\ y]^{\mathrm{T}}$ can be expressed as

$$\ln p(\tilde{\mathbf{z}}|\,\boldsymbol{l}) \propto -\frac{(N-1)}{2}\ln|\boldsymbol{\Sigma}(x,y)| - \frac{1}{2}(\tilde{\mathbf{z}}-\boldsymbol{\mu}(x,y))^{\mathrm{T}}\,\boldsymbol{\Sigma}^{-1}(x,y)\,(\tilde{\mathbf{z}}-\boldsymbol{\mu}(x,y)) \quad (52)$$

Then, the FIM, given by

$$\tilde{\mathbf{I}} = \begin{bmatrix} -\mathrm{E}\left\{\frac{\partial^2}{\partial x^2}\ln p(\tilde{\mathbf{z}}|\boldsymbol{l})\right\} & -\mathrm{E}\left\{\frac{\partial^2}{\partial x \partial y}\ln p(\tilde{\mathbf{z}}|\boldsymbol{l})\right\} \\ -\mathrm{E}\left\{\frac{\partial^2}{\partial x \partial y}\ln p(\tilde{\mathbf{z}}|\boldsymbol{l})\right\} & -\mathrm{E}\left\{\frac{\partial^2}{\partial y^2}\ln p(\tilde{\mathbf{z}}|\boldsymbol{l})\right\} \end{bmatrix} \quad (53)$$

can be obtained by first calculating the partial derivatives of the log-likelihood function in Equation (52).

For simplicity of the expressions, the (x, y) arguments in Equation (52) are omitted, and $g = |\mathbf{\Sigma}|$ and $h_{ij} = [\mathbf{\Sigma}^{-1}]_{ij}$ are defined, where $|\mathbf{\Sigma}|$ represents the determinant of $\mathbf{\Sigma}$ and $[\mathbf{\Sigma}^{-1}]_{ij}$ represents the element of $\mathbf{\Sigma}^{-1}$ in the ith row and jth column. Then, the first derivative of Equation (52) with respect to x can be calculated as

$$\begin{aligned} \frac{\partial}{\partial x}\ln p(\tilde{\mathbf{z}}|\boldsymbol{l}) = -\frac{(N-1)}{2g}\frac{\partial g}{\partial x} - \frac{1}{2}\sum_{i,j=1}^{N-1}\Bigg\{ & -\frac{\partial \mu_i}{\partial x}h_{ij}(\tilde{z}_j - \mu_j) \\ & + (\tilde{z}_i - \mu_i)\frac{\partial h_{ij}}{\partial x}(\tilde{z}_j - \mu_j) \\ & -(\tilde{z}_i - \mu_i)h_{i,j}\frac{\partial \mu_j}{\partial x}\Bigg\} \end{aligned} \quad (54)$$

For $\partial \ln p(\tilde{\mathbf{z}}|\boldsymbol{l})/\partial y$, the same expression as in Equation (54) is obtained, with the only difference being that the partial derivatives are with respect to y in that case.

After calculating the second derivative and taking the expectation, we obtain

$$\begin{aligned} \mathrm{E}\left\{\frac{\partial^2}{\partial x^2}\ln p(\tilde{\mathbf{z}}|\boldsymbol{l})\right\} = & -\frac{(N-1)}{2g^2}\left[g\frac{\partial^2 g}{\partial x^2} - \left(\frac{\partial g}{\partial x}\right)^2\right] \\ & -\sum_{i,j=1}^{N-1} h_{ij}\frac{\partial \mu_i}{\partial x}\frac{\partial \mu_j}{\partial x} \\ & -2f_N^2\sigma_N^2\sum_{i,j=1}^{N-1}\frac{\partial^2 h_{ij}}{\partial x^2} \\ & -2\sum_{i=1}^{N-1}\frac{\partial^2 h_{ii}}{\partial x^2}f_i^2\sigma_i^2 \end{aligned} \quad (55)$$

Similarly, $\mathrm{E}\left\{\frac{\partial^2}{\partial y^2}\ln p(\tilde{\mathbf{z}}|\boldsymbol{l})\right\}$ can be obtained.

The off-diagonal terms in Equation (53) can be derived after some manipulation as

$$\begin{aligned} \mathrm{E}\left\{\frac{\partial^2}{\partial x \partial y}\ln p(\tilde{\mathbf{z}}|\boldsymbol{l})\right\} = & -\frac{(N-1)}{2g^2}\left[g\frac{\partial^2 g}{\partial x \partial y} - \frac{\partial g}{\partial x}\frac{\partial g}{\partial y}\right] \\ & -\sum_{i,j=1}^{N-1} h_{ij}\frac{\partial \mu_i}{\partial x}\frac{\partial \mu_j}{\partial y} \\ & -2f_N^2\sigma_N^2\sum_{i,j=1}^{N-1}\frac{\partial^2 h_{ij}}{\partial x \partial y} \\ & -2\sum_{i=1}^{N-1} f_i^2\sigma_i^2\frac{\partial^2 h_{ii}}{\partial x \partial y} \end{aligned} \quad (56)$$

In addition, it can be shown from Equations (2) and (18) that

$$\frac{\partial \mu_i}{\partial x} = 2(x_i - x_N), \qquad \frac{\partial \mu_i}{\partial y} = 2(y_i - y_N) \quad (57)$$

Therefore, $\sum_{i,j=1}^{N-1} h_{ij}\frac{\partial \mu_i}{\partial x}\frac{\partial \mu_j}{\partial x}$ becomes equal to $4\mathbf{b}_x^{\mathrm{T}}\mathbf{\Sigma}^{-1}\mathbf{b}_x$, where $\mathbf{b}_x$ ($\mathbf{b}_y$) is as given in Proposition 1. Similarly, $\sum_{i,j=1}^{N-1} h_{ij}\frac{\partial \mu_i}{\partial y}\frac{\partial \mu_j}{\partial y}$ and $\sum_{i,j=1}^{N-1} h_{ij}\frac{\partial \mu_i}{\partial x}\frac{\partial \mu_j}{\partial y}$ become equal to $4\mathbf{b}_y^{\mathrm{T}}\mathbf{\Sigma}^{-1}\mathbf{b}_y$ and $4\mathbf{b}_x^{\mathrm{T}}\mathbf{\Sigma}^{-1}\mathbf{b}_y$, respectively.

Then, from Equations (55) to (57), the inverse of $\tilde{\mathbf{I}}$ in Equation (53) can be calculated, and the CRLB expression in Proposition 1 can be obtained. ■

APPENDIX B

Proof of Proposition 2. One way to prove the claim in the proposition is to show that there is a one-to-one mapping between the measurement sets in Equations (28) and (14). To that aim, it is first observed that each measurement in Equation (14) is simply equal to the difference of two measurements in Equation (28). Specifically, $\tilde{z}_i = \bar{z}_r - \bar{z}_i$ for $i = 1, \ldots, N-1$, where $\tilde{i}$ is as in Equation (15). Then, it can be shown that each measurement in Equation (28) can be obtained from those in Equation (14) as the difference between the average of the measurements in Equation (14) and the corresponding measurement in Equation (14). In other words,

$$\begin{aligned} \bar{z}_i = \frac{1}{N}\sum_{j=1}^{N-1}\tilde{z}_j - \tilde{z}_i &= \frac{1}{N}\sum_{j=1}^{N-1}\left(z_r^2 - z_j^2\right) - (z_r^2 - z_i^2) \\ &= \left(z_r^2 - \frac{1}{N}\sum_{j=1}^{N} z_j^2\right) - (z_r^2 - z_i^2) = z_i^2 - \frac{1}{N}\sum_{j=1}^{N} z_j^2 \end{aligned}$$

for $i = 1, \ldots, N-1$, where $r = N$ is assumed without loss of generality. Note that $\bar{z}_N$ can be obtained from $\frac{1}{N}\sum_{j=1}^{N-1}\tilde{z}_j$.

Since the measurements in the sets (14) and (28) can be obtained from each other, they carry the same amount of statistical information; hence, the CRLBs based on those measurements are the same. ■

REFERENCES

1. Caffery JJ. *Wireless Location in CDMA Cellular Radio Systems*. Kluwer Academic Publishers: Boston, 2000.

2. Gezici S. A survey on wireless position estimation. *Wireless Personal Communications* 2008; **44**(3): 263–282.
3. Sahinoglu Z, Gezici S, Guvenc I. *Ultra-wideband Positioning Systems: Theoretical Limits, Ranging Algorithms, and Protocols*. Cambridge University Press: New York, 2008.
4. Gezici S, Poor HV. Position estimation via ultra-wideband signals. *Proceedings of IEEE* 2009; **97**(2): 386–403.
5. Basagni S, Chlamtac I, Syrotiuk VR. Location aware one-to-many communication in mobile multi-hop wireless networks. In *Proceedings of IEEE Vehicular Technology Conference (VTC)*, Vol. 1, Tokyo, May 2000; 288–292.
6. Feng K-T, Lu C-T. A location and mobility aware medium access control protocol for directional antenna-based mobile ad hoc networks. In *Proceedings of IEEE Vehicular Technology Conference (VTC)*, Vol. 1, Melbourne, May 2006; 299–303.
7. Mahmood H, Comaniciu C. Location assisted routing for near-far effect mitigation in wireless networks. In *Proceedings of International Conference on Collaborative Computing: Networking, Applications and Worksharing*, December 2005.
8. Gustafsson F, Gunnarsson F. Mobile positioning using wireless networks: possibilites and fundamental limitations based on available wireless network measurements. *IEEE Signal Processing Magazine* 2005; **22**(4): 41–53.
9. Poor HV. *An Introduction to Signal Detection and Estimation*. Springer-Verlag: New York, 1994.
10. Chen P-C. A non-line-of-sight error mitigation algorithm in location estimation. In *Proceedings of IEEE International Conference on Wireless Communications and Networking (WCNC)*, Vol. 1, New Orleans, LA, September 1999; 316–320.
11. Seber GAF, Wild CJ. Nonlinear Regression, John Wiley & Sons: Auckland, New Zealand, 1989.
12. Bates DM, Watts DG. *Nonlinear Regression Analysis and Its Applications*. John Wiley & Sons: New York, 1988.
13. Kim W, Lee JG, Jee GI. The interior-point method for an optimal treatment of bias in trilateration location. *IEEE Transactions on Vehicular Technology* 2006; **55**(4): 1291–1301.
14. Caffery JJ. A new approach to the geometry of TOA location. In *Proceedings of IEEE Vehicular Technology Conference (VTC)*, Vol. 4, Boston, MA, September 2000; 1943–1949.
15. Venkatesh S, Buehrer RM. A linear programming approach to NLOS error mitigation in sensor networks. In *Proceedings of IEEE International Symposium on Information Processing in Sensor Networks (IPSN)*, Nashville, Tennessee, April 2006; 301–308.
16. Li Z, Trappe W, Zhang Y, Nath B. Robust statistical methods for securing wireless localization in sensor networks. In *Proceedings of IEEE International Symposium on Information Processing in Sensor Networks (IPSN)*, Los Angeles, CA, April 2005; 91–98.
17. Chan YT, Hang HYC, Ching PC. Exact and approximate maximum likelihood localization algorithms. *IEEE Transactions on Vehicular Technology* 2006; **55**(1): 10–16.
18. Guvenc I, Chong CC, Watanabe F. Analysis of a linear least-squares localization technique in LOS and NLOS environments. In *Proceedings of IEEE Vehicular Technology Conference (VTC)*, Dublin, Ireland, April 2007; 1886–1890.
19. Guvenc I, Chong C-C, Watanabe F, Inamura H. NLOS identification and weighted least-squares localization for UWB systems using multipath channel statistics. *EURASIP Journal on Advances in Signal Processing (Special Issue on Signal Processing for Location Estimation and Tracking in Wireless Environments)*, 2008, article ID 271984.
20. Qi Y. Wireless geolocation in a non-line-of-sight environment. *Ph.D. Dissertation*, Princeton University, December 2004.
21. Al-Jazzar S, Caffery JJ, You H-R. A scattering model based approach to NLOS mitigation in TOA location systems. In *Proceedings of IEEE Vehicular Technology Conference (VTC 2002)*, Birmingham, AL, May 2002; 861–865.
22. Gezici S, Kobayashi H, Poor HV. Non-parametric non-line-of-sight identification. In *Proceedings of IEEE Vehicular Technology Conference (VTC)*, Vol. 4, Orlando, FL, October 2003; 2544–2548.
23. Borras J, Hatrack P, Mandayam NB. Decision theoretic framework for NLOS identification. In *Proceedings of IEEE Vehicular Technology Conference (VTC)*, Vol. 2, Ontario, Canada, May 1998; 1583–1587.
24. Venkatraman S, Caffery J. A statistical approach to non-line-of-sight BS identification. In *Proceedings of 25th International Symposium on Wireless Personal Multimedia Communications*, Honolulu, HI, October 2002; 296–300.
25. Qi Y, Kobayashi H, Suda H. On time-of-arrival positioning in a multipath environment. *IEEE Transactions on Vehicular Technology* 2006; **55**(5): 1516–1526.
26. Gezici S, Guvenc I, Sahinoglu Z. On the performance of linear least-squares estimation in wireless positioning systems. In *Proceedings of IEEE International Conference on Communications (ICC)*, Beijing, China, May 2008; 4203–4208.
27. Sayed AH, Tarighat A, Khajehnouri N. Network-based wireless location. *IEEE Signal Processing Magazine.* 2005; **22**(4): 24–40.

28. Guvenc I, Gezici S, Watanabe F, Inamura H. Enhancements to linear least squares localization through reference selection and ML estimation. In *Proceedings of IEEE International Conference on Wireless Communications and Networking (WCNC)*, Las Vegas, NV, April 2008; 284–289.
29. Guvenc I, Chong CC, Watanabe F. NLOS identification and mitigation for UWB localization systems. In *Proceedings of IEEE International Conference on Wireless Communications and Networking (WCNC)*, Hong Kong, March 2007; 1571–1576.
30. Kay SM. *Fundamentals of Statistical Signal Processing: Estimation Theory*. Prentice Hall, Inc.: Upper Saddle River, NJ, 1993.
31. Mahmoud H, Arslan H, Ozdemir M. Initial Ranging for WiMAX (802.16e) OFDMA. In *Proceedings of IEEE Military Communication Conference (MILCOM)*, Washington, DC, October 2006; 1–7.

AUTHORS' BIOGRAPHIES

Ismail Guvenc received his B.S. degree from Bilkent University, Turkey, in 2001, M.S. degree from University of New Mexico, Albuquerque, NM, in 2003, and Ph.D. degree from University of South Florida, Tampa, FL, in 2006 (with outstanding dissertation award), all in Electrical Engineering. He was with Mitsubishi Electric Research Labs in Cambridge, MA, in 2005, and since June 2006, he has been with DOCOMO USA Labs, Palo Alto, CA, working as a research engineer. His recent research interests include femtocells, relay networks, LTE systems, cognitive radio, and UWB localization. He has published more than 50 conference and journal papers, and several standardization contributions for IEEE 802.15 and IEEE 802.16 standards. Dr. Guvenc continuously serves in the technical program and organizing committees of international conferences, has served as the lead guest editor for EURASIP Journal on Wireless Communications and Networking (special Issue on Femtocell Networks), workshop co-chair for IEEE Globecom 2010 Workshop on Femtocell Networks, and workshop co-chair for IEEE ICC 2011 workshop on Heterogeneous Networks. He co-authored/co-edited two books on short-range wireless communications and positioning for Cambridge University Press. Dr. Guvenc holds 4 U.S. patents, and has another 20 pending U.S. patent applications.

Sinan Gezici received the B.S. degree from Bilkent University, Turkey in 2001, and the Ph.D. degree in Electrical Engineering from Princeton University in 2006. From April 2006 to January 2007, he worked as a Visiting Member of Technical Staff at Mitsubishi Electric Research Laboratories, Cambridge, MA. Since February 2007, he has been an Assistant Professor in the Department of Electrical and Electronics Engineering at Bilkent University. Dr. Gezici's research interests are in the areas of signal detection, estimation and optimization theory, and their applications to wireless communications and localization systems. Among his publications in these areas is the book Ultra-wideband Positioning Systems: Theoretical Limits, Ranging Algorithms, and Protocols (Cambridge University Press, 2008).

Zafer Sahinoglu received his B.S. in E.E. from Gazi Uni., Ankara, M.S. in BME and Ph.D. in EE from NJIT. He was awarded the Hashimoto Prize in 2002, and the MERL President's award in 2009. He worked at AT&T Shannon Labs in 1999, and joined MERL in March 2001 where he is currently with the Digital Communications and Networking Group. His current research interests include wireless power transfer, STAP, smart grid technologies and routing dense smart meter networks. He has published more than 60 journals, book, book chapters and conference papers in the relevant topics. He has significant contributions to MPEG-21, ZigBee, IEEE 802.15.4a and IEEE 802.15.4e standards. He holds 2 European and 23 US patents. He is an IEEE senior member and and a technical editor of IEEE 802.15.4e.